

Study on freeze-thaw coupling properties of chlorine salt with cracked ultra-high performance concrete

Ouyang Dingcheng

School of Environment and Architecture, University of Shanghai for Science and Technology, Shanghai 200093

Abstract

The significant shrinkage combined with external loads often results in ultra-high performance concrete (UHPC) in a state of cracking during service. The presence of cracks can accelerate the invasion of harmful ions in the environment, thereby causing structural damage. This article sets pre tensile strain levels of 0%, 0.05%, and 0.1%, and comprehensively evaluates the chloride freeze-thaw coupling performance of UHPC by conducting uniaxial tensile, mass loss, and relative resonance frequency monitoring, silver nitrate titration, and scanning electron microscopy and energy dispersive spectroscopy (SEM-EDS) observation experiments. The results show that after freeze-thaw of chloride salts, the initial cracking strength, tensile strength, and tensile strain of the cracked specimens show a more severe decrease than those of the uncracked specimens, and the higher the level of cracking, the more significant the decrease; The relative mass and resonance frequency of the cracked specimen gradually increase with the continuous freezing and thawing of chloride salts. Even though the chloride salt coupling freeze-thaw effect, the chloride ion penetration depth and diffusion coefficient of the cracked specimen are far less than the specification requirements.

Keywords: Ultra-high performance concrete; Chlorine freeze-thaw cycle; with cracks; Uniaxial tensile properties; Relative resonance frequency; Microstructure.

Date of Submission: 05-03-2024

Date of acceptance: 18-03-2024

I. INTRODUCTION

Ultra-high performance concrete (UHPC) has been widely studied and applied because of its excellent mechanics, toughness and durability. However, lower water glue ratio and higher amount of cementing material often lead to significant UHPC contraction, combined with external load, band cracking is often inevitable. Cracking is a common phenomenon of concrete structure, the existence of cracks provides a convenient channel for the invasion of water and harmful ions, accelerate the invasion of the structure, and then cause the damage of concrete structure[1]. Secondly, after the harmful ions invade the inside of the structure, it will damage the passivation film on the surface of the steel bar, cause the steel bar corrosion, resulting in the bonding force of the steel bar and concrete greatly reduced, and then destroy the integrity of the structure.

Due to its excellent durability, UHPC has great application prospects in extreme environments. In seasonal frozen soil areas, the frost swelling effect caused by freeze-thaw cycle is the main cause of concrete structure failure[2]. However, the engineering structure in complex environment often suffers the effect of multi-factor coupling[3], Chloride erosion is one of the non-negligible destructive effects. Therefore, it is of practical engineering significance to study the performance of UHPC to resist freezing and thawing.

Some scholars have studied the resistance to chloride erosion and freezing-thaw resistance of UHPC. Pyo class[4]The chlorine salt erosion resistance of UHPC was studied by natural immersion method, and found that the bending strength of the specimen was not significantly reduced, and the corrosion of steel fiber had little influence on the compressive strength. Fan class[5]Electrochemical testing of UHPC against chloride ion erosion showed that the chloride ion did not penetrate into the matrix and did not cause reinforcement corrosion when the volume content of steel fiber in UHPC is up to 3%. Lu class[6]The influence of the influence of UHPC components on freezing resistance was explored and found that the most significant effect of water-glyce ratio, the lower the water-glyce ratio, the stronger the freezing resistance. Hua-di zhang[7]A study on the compressive and folding strength of polycarbon nanotube UHPC under the influence of composite salt (bicarbonate, chloride salt and sulfate), and found that the greater the concentration of erosion solution, the more serious the damage of frost biave. Lv class[8]We analyzed the chloride permeability of band cracked UHPC placed in the Marine environment, and found that the chloride permeability of band cracked UHPC in the Marine environment was much greater than that of indoor high concentration immersion environment, and the chloride permeability increased with the increase of damage level. In conclusion, it can be seen that the existing research on UHPC chloride resistance and freezing resistance have gradually developed from single environment factor to multi-environment coupling, and the durability study in band crack state has attracted the attention of scholars

because it is closer to the actual service state.

This paper studies the coupling properties of chapped UHPC to provide theoretical support for promoting UHPC in extreme environments. Based on the uniaxial tensile test, three specimens with different precrack levels (0%, 0.05% and 0.1%) were designed for chloride freeze-thaw cycle test. The coupling properties of UHPC is comprehensively evaluated by uniaxial tensile properties (primary crack strength, tensile strength and tensile strain), relative mass, resonance frequency, chloride concentration and diffusion coefficient. Finally, the microstructure and product changes of UHPC under chloride freeze-thaw coupling were analyzed using the SEM-EDS technique.

1.1 Raw materials, and mix ratio

Prepare UHPC from PII 52.5 ordinary Portland cement, silica ash, river sand, steel fiber, water reducing agent and water. The chemical composition of cement and silica ash is shown in Table 1. The maximum grain size of the river sand is less than 1.25 mm. Steel fiber uses two kinds of flat type copper plated steel fiber to improve UHPC and tensile properties[9], Its diameter and length are 0.2 mm and 13 / 18 mm, respectively, and the volume content is 2.5% (1.5% and 1.0% respectively). Water reducing agent selects liquid high-performance polycarboxylic acid water reducing agent with water reduction rate higher than 30%. The water is based of local tap water. The specific mix ratio is shown in Table 2.

Table1 Chemical components of cement and silica fume

Material	Mass fraction/wt %								
	SiO2	Al2O3	Fe2O3	CaO	MgO	SO3	Na2O	K2O	LOI
Cement	19.3	3.8	3.4	63.5	2.8	3.5	0.1	0.8	1.44
Silica fume	93.0	0.3	0.8	0.3	0.3	0.8	0.36	-	1.5

Table2 Mixture proportion of ultra-high performance concrete (UHPC) with hybrid fibers (wt %)

Cement	Silica fume	Sand	Water	Superplasticizer	Steel fibers	
					Long	Short
36.88	6.15	40.98	8.18	0.29	4.58	3.06

1.2 Preparation and curing of test specimens

Choose STWJ-60 concrete horizontal mixer and stir according to the following process: (1) add dry material (cement, silica ash and sand) to the mixer to make the dry material mix evenly; (2) mix water and water reducing agent and add to the dry material for 5 min to make the slurry liquid; (3) add steel fiber, fast mixing for 5 min, make the fiber evenly dispersed and stop stirring. Quickly cast the fresh concrete into the mold corresponding to different tests, and place the vibration table for about 30s. Then, cover the specimen with plastic film and place it in the laboratory at normal temperature (temperature is $20 \pm 3^\circ\text{C}$, humidity is $75 \pm 5\%$) for 24 h, remove the mold, and continue the curing at normal temperature for 28 d.

1.3 Test method

After the maintenance, the WDW-300 electronic universal testing machine produced by Jinan Chuanbai Instrument and Equipment Co., Ltd. is used for pre-crack treatment at different tensile strain levels. The specimen is dog bone shape with standard spacing of 100 mm and standard cross section of 50 mm 50 mm (see Figure 1 for detailed dimensions). A set of displacement sensors (LVDT) is fixed on each side of the specimen to measure the length change of the standard section to calculate the tensile strain. Based on the previous shrinkage test results (about 0.08%), the preloaded tensile strain levels studied in this paper were set to 0% (reference), 0.05% and 0.1%.

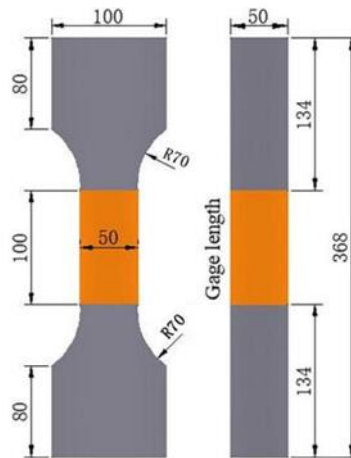
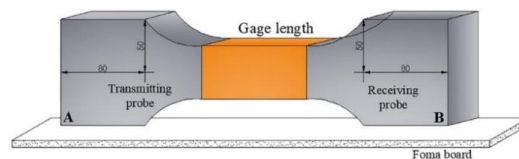


Fig.1 Uniaxial tensile test: Geometry of the dog-bone specimen

According to the GB / T 50082-2009[10]The rapid freeze-thaw cycle test of chlorine salt with cracked UHPC was conducted to determine the coupling properties of chlorine salt resistance. Each cycle temperature varies at-17-5 °C for approximately 6 cycles per day for a total of 600 cycles (replace the chloride solution every 100 cycles). The mass and resonance frequency of the specimen were measured every 100 cycles (note: the specimen was removed 1 d in advance and left in air for 1 d before measuring). The resonance frequency of the dog bone specimen was measured using a resonance frequency tester, and the test device is shown in Figure 2. The entire device consists of an emitting probe, a receiving probe, and a digital display. To minimize environmental interference, the dog bone specimen was placed on the foam plate for measurement.



(a)



(b)

Fig .2 I ll ustration of resonant frequency measurement : (a) test setup, (b) measure d position

After the end of 450 and 600 cycles, the specimens were subjected to a uniaxial tensile test with a loading rate of 0.3 mm / min, and three parallel specimens were tested in each group. SEM-EDS was used to observe the interface structure and fracture changes of the fiber and the matrix before and after freeze-thaw.

After the end of 600 cycles, according to the Technical Specification for Detection of Chloride Content in Concrete[11], Choose the test method of water-soluble chloride ion content in hardened concrete for the chloride ion concentration test. The chloride diffusion coefficient and surface chloride concentration were fitted by Fick's second law.

II. RESULT AND DISCUSSION

2.1 Tensile properties

The tensile stress-strain curves of different UHPC specimens after chlorine freeze-thaw cycle are shown in Figure 4. The parameters such as the initial crack strength (turning point stress in the elastic and hardened segments of the curve), the tensile strength (ultimate stress) tensile strain (strain corresponding to the ultimate stress) are summarized in Figure 5.

After 600 chloride freeze-thaw cycles, the initial crack strength of the uncracked specimen (0% -600C) was 7.86 MPa, 2.9% higher compared with that before freeze-thaw. This is mainly attributed to the rehydration effect of the matrix[13]. The very low water-to-glue ratio determines the residue of more unhydrated components in the UHPC base. After contact with water again, UHPC can still occur secondary hydration even at low temperature, thus improving the compactness of the matrix[14], This may compensate for the damage to the matrix by freezing and thawing, resulting in a slight increase in the initial fissure strength[38].

Due to the secondary hydration effect of the matrix, the primary crack strength of the precracked 0.05% UHPC specimens was higher than that of the uncracked specimens before freeze-thaw, confirming the self-healing of UHPC at low temperature

The initial crack strength of the split specimen first increases and then decreases with the increase of the freeze and thaw cycles, and the higher the precrack level, the more significant the decrease of the initial crack strength. The primary crack strength of both split specimens (0.05% and 0.1%) increased by 9.69% vs 2.09% at 450C and 5.24% vs 14.7% at 600C. During the crack self-healing process, the smaller the crack width, the greater the degree of self-healing[16]Therefore, the self-healing degree of 0.05% level specimen is better than 0.1% specimen, resulting in the initial crack strength of 0.05% specimen is higher than 0.1% specimen.

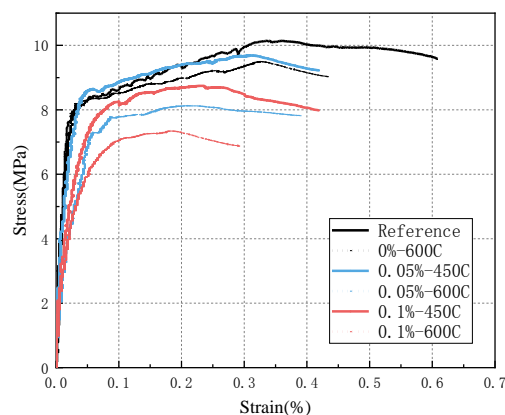


Fig.4 Tensile stress-strain curves of UHPC undergoing different chloride freeze-thaw environment actions

As can be seen from Figure 5 (b-c), chlorine freeze-thaw disruption has obvious negative effects on the tensile strength and tensile strain of UHPC, with more significant negative effects with the increase of precrack level. After 600 freeze-thaw cycles, the tensile strength of uncracked specimens, 0.05% and 0.1% were 0.52 MPa, 8.13MPa and 7.34MPa corresponding tensile strains were 0.32%, 0.21% and 0.18%, respectively. Compared to the reference specimen, the tensile strength and tensile strain of the 0% -600C specimen decreased by 5.74% and 12.5%, respectively, while the tensile strength and tensile strain of 0.05% -600C and 0.1% -600C decreased by 19.5% vs 29.2% and 41.67% vs 47.22%, respectively. The tensile performance of UHPC after cracking is related to the ability of fiber bridging at the crack, and the binding ability of the fiber-matrix interface is the key factor affecting the bridging ability[17]. Water penetrates from the pores between the surface steel fiber and the matrix, and the freezing and swelling failure of the pores reduces the bonding force between the fiber and the matrix, which is the main reason why the freezing and thawing cycle affects the tensile performance of the specimen after cracking. Notably, the effect of chlorine salt freeze-thaw on the tensile strength and tensile strain of the split specimens was more significant after 450 cycles. The tensile strength of 0.05% -450C and 0.05% -600C specimens decreased by 4.34%vs19.5% and the tensile strain by 13.89%vs41.67%, respectively. Similar changes were also found in 0.1% of the specimens, and the decrease was greater. This phenomenon is mainly attributed to the differences between the freezing temperature and expansion rate of chlorine solution in the pore in different pore sizes. Generally speaking, the freezing temperature of chlorine solution in the large pore is higher, less freezing time, the expansion rate is greater, and the damage degree of chlorine solution to the pore structure is higher[15]. As the freeze-thaw cycle continues, the porosity of the large pore size is higher, and the effect of chloride freeze-thaw disruption on reducing the fiber-matrix binding ability is more obvious. Second, the findings of previous studies[18]After 10 weeks of chloride erosion, the steel fiber will pull out, and part of the steel fiber will break, because the moderate corrosion of the steel fiber will improve the surface roughness and have a positive impact on the bonding performance of the fiber-matrix. Therefore, with the continuous development of chlorine salt freeze-thaw cycle, the influence of steel fiber corrosion on tensile properties gradually changes from positive to negative, which

makes the decrease of tensile strength and tensile strain more obvious after 450 cycles.

It can be seen that UHPC exhibits strain-stiffening behavior regardless of the precrack lesion. The tensile strain could still exceed 0.2% in 0.05% specimens after 600 cycles, while the tensile behavior of 0.1% specimens decreased significantly after 600 cycles. According to the literature[39]In the proposed UHPC tensile classification standard, after 600 chlorine freeze-thaw, the uncracked specimens is A-grade (tensile strength> 8MPa; primary crack strength> 5.5MPa; tensile strain> 0.2%), indicating that the uncracked UHPC has excellent resistance[12]

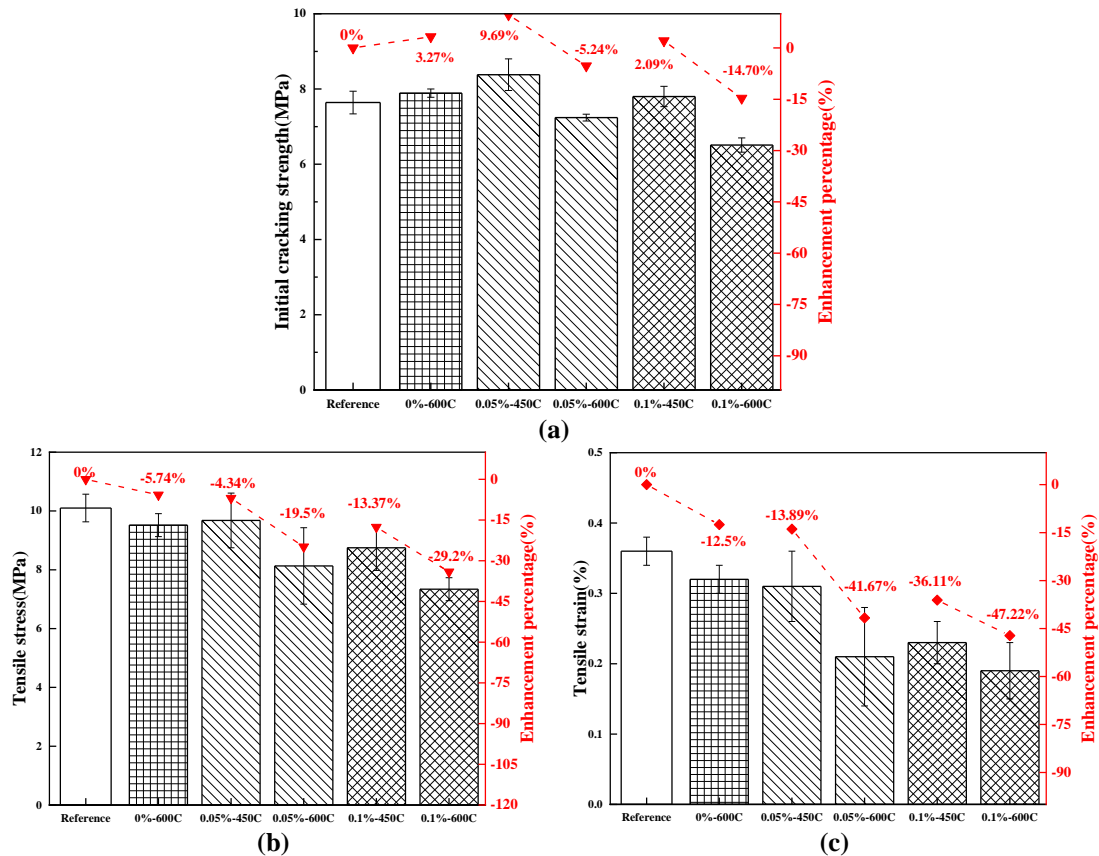


Fig.5 Tensile properties of UHPC undergoing different chloride freeze-thaw environment actions:(a) initial cracking strength;(b) tensile stress;(c) tensile strain

2.2 The cracking characteristics of UHPC

The number of cracks on the surface of different specimens after stretching is then counted according to Equations (1) and (2)[19]The average crack width and average cracking spacing were calculated separately, and the results are listed in Table 3.

Table 3 Tensile crack characteristics of the UHPC specimens

Samples	Number of cracks (-)	Average crack width (μm)	Average crack space (mm)
Reference	18±2	20.38±3.38	5.57±0.31
0%-600C	12±1	26.99±3.91	8.39±0.70
0.05%-450C	11±1	28.83±7.17	9.17±0.83
0.05%-600C	7±1	32.08±14.58	14.58±2.08
0.1%-450C	8±1	29.68±7.46	12.70±1.59
0.1%-600C	3±1	50.00±30.00	37.50±12.50

The fracture characteristics of the specimen after tensile failure can reflect the tensile properties of the material, so the fracture characteristics are also an important index parameter. It can be seen that UHPC specimens with different pre-crack levels have saturated multi-seam cracking ability. With the increase of pre-crack level and freeze-thaw cycles, the number of UHPC specimens is less and less after tensile test, indicating that pre-loading and chlorine freeze-thaw destruction weaken the multi-seam cracking capacity of UHPC.

The number of cracks, average crack width and average crack spacing of UHPC specimens after tensile failure are shown in Table 3. It can be seen that the average number of cracks in the reference specimen is 18. Different from the single-crack cracking mode, the multi-crack cracking mode can significantly improve the tensile strain of the material, and the average crack width of the reference specimen is only 20.38 μ m, which is lower than Zhang, etc[20,21]Study ECC mean crack width (50 μ m) and Kan et al[22]The crack width (25 μ m) of the investigated composite limits the penetration of the solution in the chloride freeze-thaw environment. Uncracked specimens (0%) still showed good multi-crack cracking ability after 600 chlorine salt freeze-thaw cycles, and the number of cracks was 12 after the cycle. Compared with 0% -600C specimens, the 0.05% -600C increased by 18.85% and 73.78% for 600C specimens, and the corresponding values of 0.1% -600 C increased by 85.25% and 346.96%, respectively. Meanwhile, the number of cracks in 0.05% -600C and 0.1% -600C specimens was significantly reduced by 7 and 3 pieces, respectively. It shows that after specimen preloading, the crack cracking ability and fiber expansion, and the higher the precrack level, the more significant the adverse effect.

2.3 Relative quality

Figure 6 shows the relative mass changes under the chloride freeze-thaw cycle. After the cycle, there will be a small amount of water in the internal connected hole. In order to reduce the effect of pore water on the quality, the mass is measured after every 100 cycles and after 24 h of standing in the room.

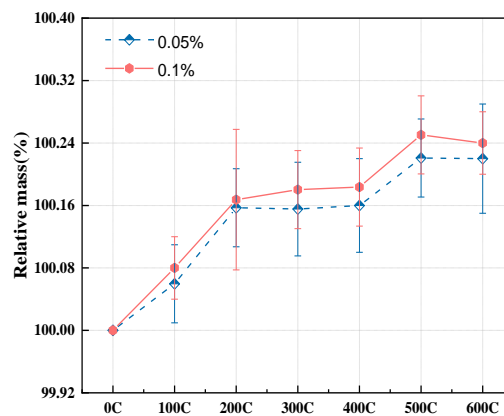


Fig.6 Changes in relative mass of different UHPC specimens

The mass increase showed, and the relative mass increase of 0.1% specimens was higher than 0.05% specimens (100.17% vs 100.16%). The water absorbed in the process of freezing and thawing reacts with the unhydrated gel material inside the material, and the secondary hydration product fills the pores, which improves the quality and reduces the deterioration. The different levels of pre-crack lead to the difference of the damage degree of the specimen. The higher the pre-crack level, the more obvious the damage degree of the specimen surface, the number and width of micro-cracks will increase accordingly, which promotes the entry of water and improves the degree of secondary hydration, resulting in the higher the level of the specimen, the more obvious the quality improvement. Related studies have also confirmed this phenomenon[23].

With the increasing chloride freeze-thaw cycle, the relative mass of the band-split test piece was placed at almost the same level between 200 and 400 cycles. This shows that after 200 chlorine freeze-thawing cycles, the rehydration effect on the defect has been greatly weakened, and the dense matrix and very low porosity of UHPC make it have excellent freezing resistance properties, so the freezing-thawing effect has little impact on the quality damage[24-27]. Between 400-500 cycles, the mass of the split test suddenly rises, this is because the damage of frost effect on the pore structure, the increase of porosity improves the water content of the matrix, and the air for 24 h can not completely exclude the residual water in the pore, leading to the improvement of the relative quality. After the end of 600 freeze-thaw cycles, the relative mass of the split specimen decreased compared with the mass of 500C, and the mass of 0.1% -600C specimens decreased more. The peeling of surface mortar and steel fiber is the main reason for the mass decline, while the higher precrack level leads to more serious damage.

2.4 Relative resonance frequency

The relative resonance frequencies of the UHPC specimens in each test phase are shown in Figure 7.

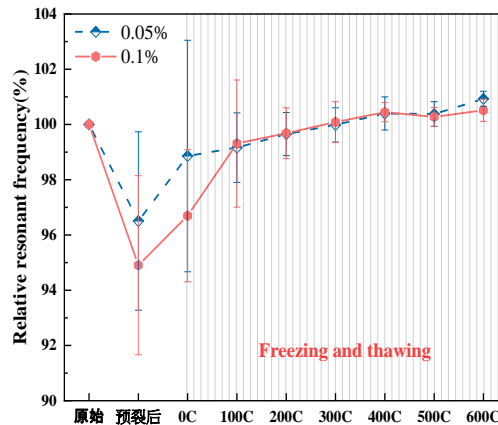
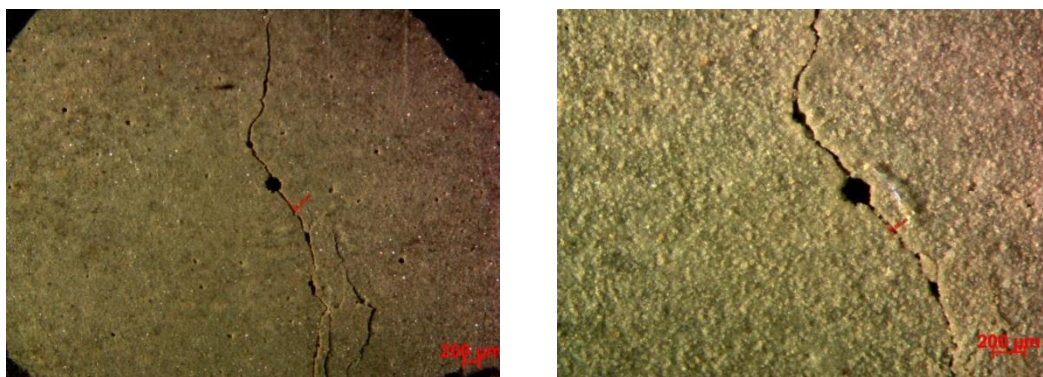


Fig.7 Relative resonant frequency of different UHPC specimens

Resonance frequency is an effective indicator to characterize the degree of damage inside the specimen[28]. After preloading of UHPC, the production of microcracks caused a decrease in resonance frequency, and the magnitude of the decrease was positively correlated with the level of damage. Due to the epidemic in Shanghai at the beginning of 2022, the split specimen was placed outdoors for up to 6 months. Before the start of chlorine freeze-thaw cycle, the resonance frequency of each specimen was re-measured. The results found that the resonance frequency of the split specimen increased. It is evident from Figure 8 that white powder appears at the crack of the 0C specimen because of outdoor moisture and CO₂ in the air in summer. Into the material through the microcrack, with the hydration product Ca(OH)₂ reaction occurs, and the resulting CaCO₃ partially fills the crack[29]. Increase in resonance frequency. Graybeal[30]The study found that UHPC also has self-healing in air, which also supports the reliability of increased resonance frequency.

In the process of chloride freeze-thaw cycle, the resonance frequency of the split specimen increased significantly after the end of 100 cycles, and the higher the increase in the resonance frequency was the crack defect, and the higher the resonance frequency increased (0.05% vs 0.1%: 0.3% vs 2.62%). With the increase of freezing and thawing cycle, the resonance frequency still increases steadily. After the end of 450 cycles, the resonance frequency of the split specimen is greater than the reference specimen, and this change rule is inconsistent with the law of the initial crack strength (at 450C, the tensile performance of the split specimen is significantly decreased). The reason is that the primary crack strength reflects the compactness of the matrix, which is also associated with the degree of damage on the surface, while the resonance frequency mainly reflects the compactness inside the material. At 450 cycles, the surface of the split specimen has been peeled off, which has a negative impact on the initial crack strength of the material. At 500C and 600C compared with 400C, and the damage of the chlorine freeze-thaw environment destroyed the pore structure.



(a) After pre-cracking

(b)0C(180d)

Fig.8 Tensile crack characteristics of the UHPC

2.5 cut face structure

The distribution of the pores inside the concrete will affect the service life of the structure. As an important part of UHPC, steel fiber can significantly improve the mechanical properties of UHPC. However, the pores at the fiber-matrix interface can increase the corrosion risk of steel fibers[31], Moreover, changes in pore structure may also increase the risk of erosive ion erosion, infiltrating into the material and thus affecting durability[32].

The failure effect of pore swelling caused by freezing and thawing cycle is the main cause of structural failure. After freezing and thawing cycle and the failure of ordinary concrete, the microscopic hole (nanopore) structure of the material is often used. Unlike ordinary concrete, when UHPC experiences freeze-thaw cycle destruction, most of the solutions in the pores do not freeze due to the supercooling effect, and only the water in the large pores can freeze[15]At the same time, the chloride ion will reduce the expansion rate of the solution, and then reduce the damage effect. In conclusion, it is of great significance to determine the change law of macroscopic pores (micron pores) in the environment of chloride freezing and thawing coupling. The section and hole information were analyzed with the image analysis and processing software ImageJ, and the aperture analysis results are shown in Figure 9.

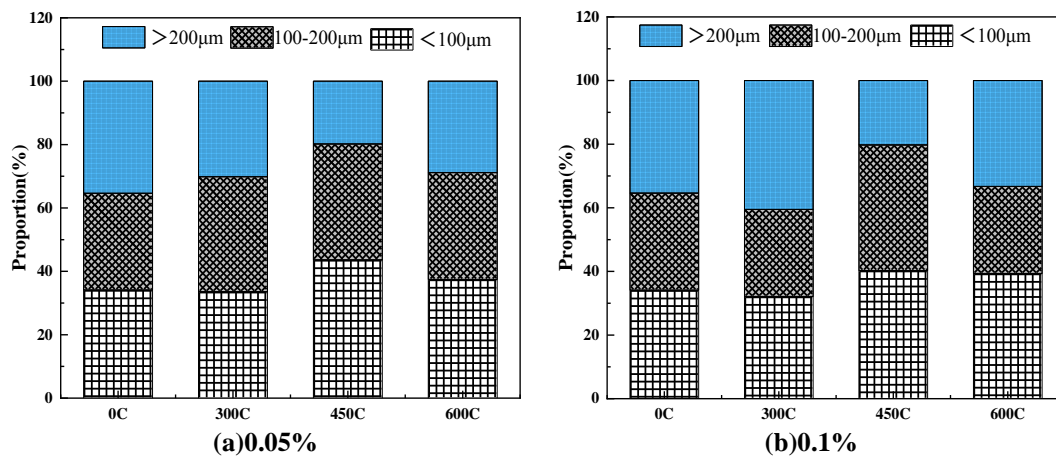


Fig.9 The pore proportion with different pore size

2.6 Degree of chloride ion erosion

The split UHPC specimens measured chloride concentrations at different depths after 600 chloride freeze-thaw cycles, and the results are shown in Figure 10. The chloride concentration of 0.1% specimen at 14 mm depth from the specimen surface is 0.22%, 5 times that of 0.05% specimen. Different precrack levels have a significant effect on the chloride concentration on the specimen surface, and higher precrack levels correspond to more microcracks, which provides favorable conditions for chloride penetration. Affected by the crack width and depth, 5-8 mm from the specimen surface, chloride ion concentration greatly reduced, dense microstructure hindered the chloride ion penetration, at the same time, the secondary hydration reaction promotes the physical adsorption and chemical chloride and hydration products, and reduces the content of free chloride ions in the pore solution, inhibit the chloride ion penetration rate. The chloride concentration of the two pre-damaged specimens at 13-16 mm from the surface was 0.004% and 0.009%, respectively, which are well below the standard[10]The required 0.06%.

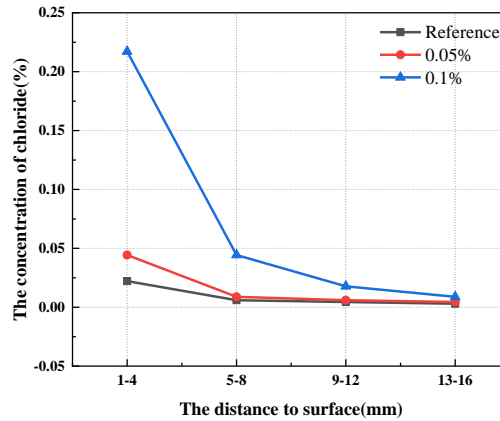


Fig.10 The chloride ion concentration distributions

2.7 chloride ion diffusion coefficient

After measuring the chloride concentration at each depth of the split specimen, the chloride diffusion coefficient and surface chloride concentration were deduced by Fick's second law. The fitting results are shown in Figure Figure 11. Three relevant parameters, including Cs (surface chloride concentration), D (chloride diffusion coefficient) and R, are obtained from Fig2. R2Represents the curve fit, the closer to 1, the higher the fit. R of the fitted curves for two split specimens20.942 and 0.987, respectively, indicating a high fit, so which Cs and D have high reliability. The chloride ion diffusion coefficient of 0.05% and 0.1% specimens was 2.09 mm²/d vs 2.14 mm²/ D, the precrack level affects the chloride diffusion coefficient, which is similar to the rule of chloride concentration. In conclusion, the band cracked UHPC specimens has excellent properties against chloride ion erosion under chloride freeze-thaw cycle conditions.

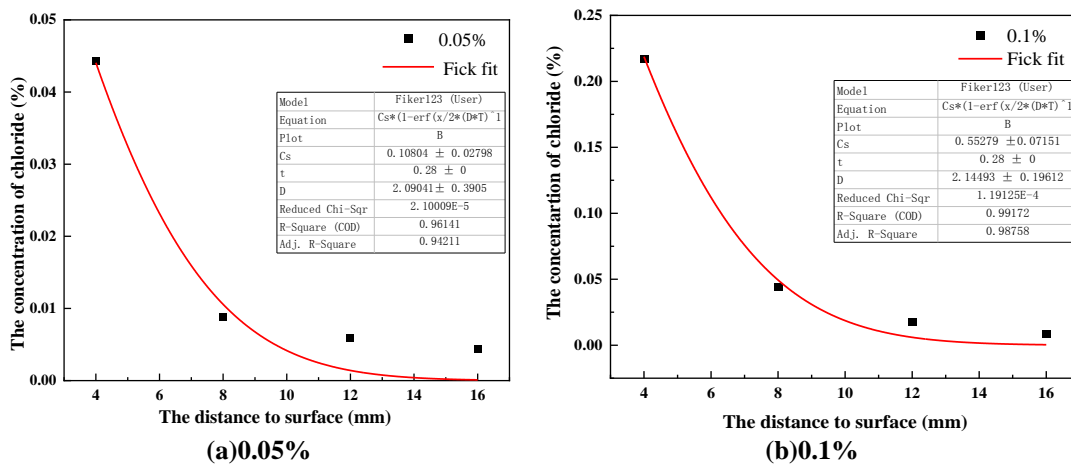


Fig.11 The diffusion coefficient

2.8 Microstructure

Figure 12 (a-b) shows the micromorphology of UHPC matrix before and after 600 chloride freeze-thaw, Figure 12 (c-d) shows the fiber-matrix bond morphology of 0.1% specimens before and after chlorine freeze-thaw, and Figure 12 (e) shows the characteristics of UHPC microcracks after chlorine freeze-thaw cycle. The results of the EDS element analysis are shown in Table 4.

The comparison of Figure 12 (a) and (b) shows that the microstructure of the matrix before the freeze-thaw cycle is dense, and the aggregate is tightly bound to the hydration product. There is no obvious damage after 600 chloride freeze-thaw cycles. Figure 12 (c) shows that there are microcracks in the base body of 0.1% of the specimens before the chlorine freeze-thaw cycle, which occurs during the precracking of UHPC. At the same time, it can be seen that there is no obvious gap between the fiber-matrix, and the bond between the two is relatively close. After 0.1% specimens underwent 600 freeze and thaw cycles, and large pores were generated between the fibers (Figure 12 (d)), the loose bonding interface had a large negative impact on tensile properties, resulting in a decrease in tensile stress and tensile strain, which reasonably explains the change in tensile properties in Section 2.1. From Figure 12 (e), it can be found that there are hydration products in the

crack, and the local cracks are repaired, which indicates that in the chlorine salt freezing-thawing environment, the unreacted cementing material can still carry out hydration reaction, but due to the damage of frost swelling, the newly generated hydration products cannot completely repair the crack.

Table4 The analyzed results of elements by EDS

Element		O	Al	Si	Cl	K	Ca	Na	Total
Area	wt %	15.50	3.41	37.10	0.74	1.60	39.55	2.10	100
	at %	27.38	3.57	37.87	0.59	1.16	27.88	1.56	100

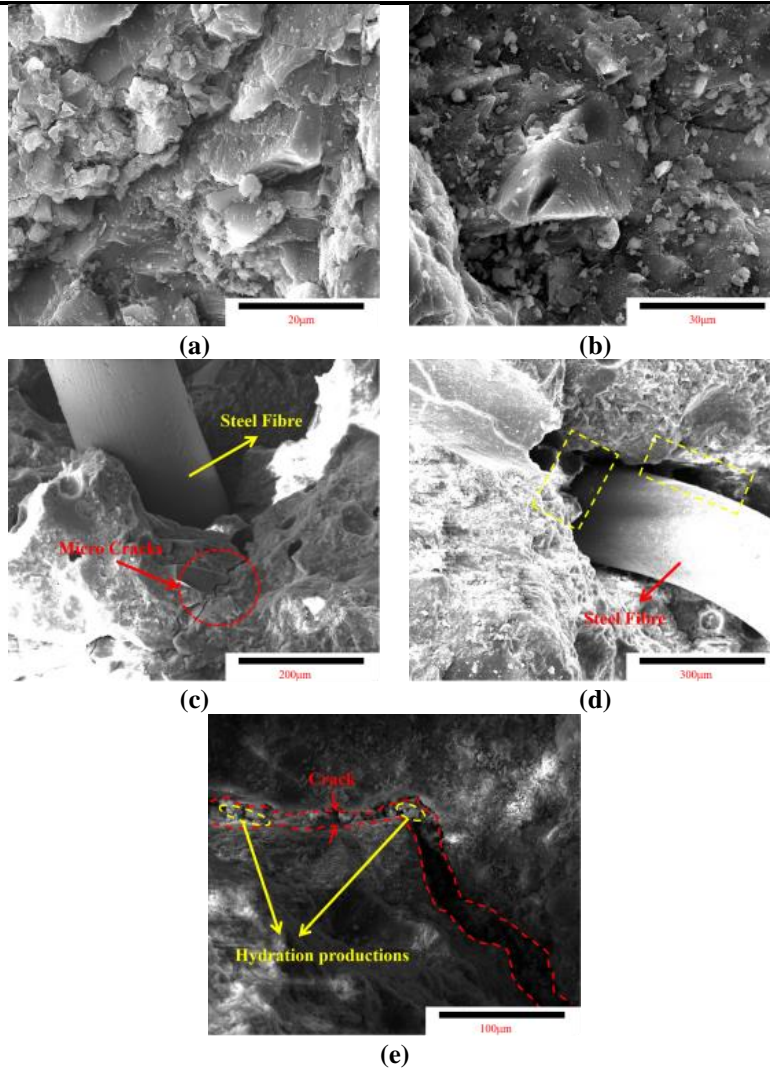


Fig.12 SEM images of Samples:(a)matrix before 600 freeze-thaw cycles of chloride salts;(b)matrix after freeze-thaw cycle of chloride salts;(c)the fiber-matrix bond morphology of 0.1% specimens before freeze-thaw cycle of chloride salts;(d)the fiber-matrix bond morphology of 0.1% specimens after 600 freeze-thaw cycles of chloride

III. INTRODUCTION

The freeze-thaw resistance of cracked ultra-high performance concrete (UHPC) was systematically investigated. 0.05% and 0.1% were generated, and the pre-cracking resistance of the specimen after 600 chlorine freeze-thaw cycles was studied. The research contents include: the primary crack strength, elastic modulus, tensile strain, tensile strength, relative resonance frequency, relative mass and face structure; the concentration of chloride concentration at different depths from the surface of the test specimen by Fick's second law; finally, the microstructure of the material is analyzed by SEM-EDS. The main conclusions are summarized as follows:

(1) With the increase of chlorine salt freeze-thaw cycle, the tensile performance of UHPC gradually decreased. After 600 cycles, the tensile stress and tensile strain were 9.52MPa and 0.32%, respectively. The pre-tensile stress and tensile strain of 0.05% and 0.1% specimens were 8.13MPa and 7.15MPa and 0.21% and 0.12%, respectively, and the tensile performance decline of the split specimens was significantly higher than that of the uncracked specimens, and the higher the pre-cracking level, the more significant the damage effect of chlorine salt.

(2) After the end of 600 chloride freeze-thaw cycles, the relative mass and resonance frequency of 0.05% and 0.1% split specimens were increased compared with the reference specimens. The rehydration reaction in the early stage increased the matrix compactness and increased both the mass and the resonance frequency. However, with the freeze-thaw cycle, the relative mass and resonance frequency started to decrease at 500C and 400C, respectively.

(3) Through the analysis of cut face structure, it can be found that with the increase of chloride freezing and thawing cycle, the aperture structure changes significantly, developing from small aperture to large aperture, which is consistent with the law of tensile performance. The results of chloride ion penetration depth and diffusion coefficient show that the split specimen still has excellent resistance to chloride ion erosion. The chlorine salt freeze-thaw cycle destroys the interface bonding properties of the fiber-matrix; the secondary hydration product can only partially repair the crack.

REFERENCES

- [1]. Pease B, Geiker M, Stang H, et al. The design of an instrumented rebar for assessment of corrosion in cracked reinforced concrete[J]. *Materials and Structures*, 2011, 44(7): 1259-1271.
- [2]. Fei Wang, Lili Kan, Jiangtao Yu, et al. Systematic studies on behaviors of ultra-high performance concrete subject to freezing and thawing cycles combining DIC technology[J]. *Construction and Building Materials*, 2023, 388: 131580.
- [3]. Liu Zhiyong, Xia Xizhi, Zhang Yunsheng, the damage behavior of ultra-high performance concrete under the action of equal load-temperature coupling [J]. *Journal of Silicate*. 2021, 49(06): 1238-1246.
- [4]. Liu Zhiyong, Xia Xizhi, Zhang Yunsheng, et al. Damage Behavior of Ultra-High Performance Concrete under Load-Temperature Coupling[J]. *Journal of the Chinese Ceramic Society*. 2021, 49(06): 1238-1246(in Chinese).
- [5]. Pyo S, Koh T, Tafesse M, et al. Chloride-induced corrosion of steel fiber near the surface of ultra-high performance concrete and its effect on flexural behavior with various thickness[J]. *Construction and Building Materials*, 2019, 224: 206-213.
- [6]. Fan L, Meng W N, Teng L, et al. Effects of lightweight sand and steel fiber contents on the corrosion performance of steel rebar embedded in UHPC[J]. *Construction and Building Materials*, 2020, 238: 117709.
- [7]. Lu Z, Feng Z G, Yao D D, et al. Freeze-thaw resistance of Ultra-High performance concrete: Dependence on concrete composition[J]. *Construction and Building Materials*, 2021, 293: 123523.
- [8]. Zhang, durability test of ultra-high performance concrete (MWCNTs-UHPC) under composite salt penetration-freeze-thaw coupling environment [D]. Changzhou University. 2022.
- [9]. Lv L S, Wang J Y, Xiao R C, et al. Chloride ion transport properties in microcracked ultra-high performance concrete in the marine environment[J]. *Construction and Building Materials*, 2021, 291: 123310.
- [10]. Kan Lili, Wang Fei, Wu Haijiang, other early age mechanical properties and cracking characteristics of mixed steel fiber ultra-high performance concrete under different curing conditions [J]. *Journal of Silicate*, 2022, 50 (2): 429-437.
- [11]. Kan Lili, Wang Fei, Wu Haijiang, et al. Mechanical Properties and Cracking Characteristics of UHPC with Hybrid Steel Fibers at Early Age under Different Curing Conditions[J]. *Journal of the Chinese Ceramic Society*, 2022, 50(2): 429-43(in Chinese).
- [12]. GB / T 50082-2009. Standard for mechanical properties and durability of ordinary concrete [S]. Beijing: China State Engineering and Construction Press, 2009.
- [13]. GB/T 50082-2009. Standard for test methods of long-term performance and durability of ordinary concrete[S]. Beijing: China Architecture & Building Press, 2013(in Chinese).
- [14]. JGJ / T 322-2013. Technical Specification for detection of chloride ion content in concrete [S]. Beijing: China State Engineering and Construction Press, 2013.
- [15]. JGJ/T 322-2013. Technical specification for test of chloride ion content in concrete[S]. Beijing: China Architecture & Building Press, 2013(in Chinese).
- [16]. Guo J Y, Wang J Y, Wu K. Effects of self-healing on tensile behavior and air permeability of high strain hardening UHPC[J]. *Construction and Building Materials*, 2019, 204: 342-356.
- [17]. Kan L L, Wang F, Zhang Z, et al. Mechanical properties of high ductile alkali-activated fiber reinforced composites with different curing ages[J]. *Construction and Building Materials*, 2021, 306: 519-527.
- [18]. Kim S, Yoo D Y, Kim M J, et al. Self-healing capability of ultra-high-performance fiber-reinforced concrete after exposure to cryogenic temperature[J]. *Cement and Concrete Composites*, 2019, 103335.
- [19]. Durability study of active powder concrete under freezing and thawing cycle and erosion [D]. Beijing Jiaotong University, 2017.
- [20]. Wang Yue. Durability of reactive powder concrete under the action of chloride salt freeze-thaw cycling and erosion[D]. Beijing Jiaotong University, 2017(in Chinese).
- [21]. Jiang J Y, Zheng X J, Wu S P, et al. Nondestructive experimental characterization and numerical simulation on self-healing and chloride ion transport in cracked ultra-high performance concrete[J]. *Construction and Building Materials*, 2019, 198: 696-709.

- [22]. Yoo D Y, Shin W, Chun B, et al. Assessment of steel fiber corrosion in self-healed ultra-high-performance fiber-reinforced concrete and its effect on tensile performance[J]. *Cement and Concrete Research*, 2020, 133: 106091.
- [23]. Yoo D Y, Gim J Y, Chun B. Effects of rust layer and corrosion degree on the pullout behavior of steel fibers from ultra-high-performance concrete[J]. *Journal of Materials Research and Technology-JMR and T*, 2020, 9(3): 3632-3648.
- [24]. Wille K, Naaman A E, Parra-Montesinos G J. Ultra-High Performance Concrete with Compressive Strength Exceeding 150 MPa (22 ksi): A Simpler Way[J]. *ACI materials journal*, 2011, 108(1): 46-54.
- [25]. Zhang Z G, Ding Y Z, Qian S Z. Influence of bacterial incorporation on mechanical properties of engineered cementitious composites (ECC)[J]. *Construction and Building Materials*, 2019, 196: 195-203.
- [26]. Zhang Z G, Yang F, Liu J C, et al. Eco-friendly high strength, high ductility engineered cementitious composites (ECC) with substitution of fly ash by rice husk ash[J]. *Cement and Concrete Research*, 2020, 137: 106200.
- [27]. Kan L L , Wang W S, Liu W D, et al. Development and characterization of fly ash based PVA fiber reinforced Engineered Geopolymer Composites incorporating metakaolin[J]. *Cement and Concrete Composites*, 2020, 108: 103521.
- [28]. Granger S, Loukili A, Pijaudier -Cabot G, et al. Experimental characterization of the self-healing of cracks in an ultra high performance cementitious material: mechanical tests and acoustic emission analysis[J]. *Cement and Concrete Research*, 2006, 37(4): 519-527.
- [29]. Peng Y, Zhang J, Liu J, et al. Properties and microstructure of reactive powder concrete having a high content of phosphorous slag powder and silica fume[J]. *Construction and Building Materials*, 2015, 101: 482-487.
- [30]. Dils J, Boel V, De Schutter G. Influence of cement type and mixing pressure on air content, rheology and mechanical properties of UHPC[J]. *Construction and Building Materials*, 2013, 41: 55-463.
- [31]. Aitcin P C. The durability characteristics of high performance concrete: A review[J]. *Cement and Concrete Composites*, 2003, 25(4): 409-420.
- [32]. Colombo L G, Colombo M, Di Prisco M. Tensile behavior of textile reinforced concrete subjected to freezing-thawing cycles in un-cracked and cracked regimes[J]. *Cement and Concrete Research*, 2015, 73: 169-183.
- [33]. Nguyen H H , Choi J I, Song K I, et al. Self-healing properties of cement-based and alkali-activated slag-based fiber-reinforced composites[J]. *Construction and Building Materials*, 2018, 165: 801-811.
- [34]. Tan Yu, Lu Liang Sheng, Wang Junyan, et al. Rapid healing mechanism of UHPC microcracks in the vapor environment [J]. *Highway Journal of China*, 2021, 34 (08): 55-64.
- [35]. TAN Yu, Lv Liangsheng , Wang Junyan , et al. Rapid Healing Mechanism of UHPC Microcracks in a Steam Environment[J]. *China Journal of Highway and Transport*, 2021, 34(08): 55-64(in Chinese).
- [36]. Graybeal B A. Material property characterization of ultra-high performance concrete[R]. No. FHWA-H RT-06-103, 2006.
- [37]. Reddy B, Glass G, Lim P, et al. On the corrosion risk presented by chloride bound in concrete, *Cement and Concrete Composites*, 2002, 24(1): 1-5.
- [38]. Hwang J P, Kim M, Ann K Y. Porosity generation arising from steel fiber in concrete[J]. *Construction and Building Materials*, 2005, 94: 433-436.
- [39]. Fei Wang, Lili Kan, Jiangtao Yu, Xin -Zhi Duan. Systematic studies on behaviors of ultra-high performance concrete subject to freezing and thawing cycles combining DIC technology[J]. *Construction and Building Materials*, 2023, 388: 131580.
- [40]. Chen Baochun, Yang Jian, Wu Xianguo, et al. Multi-index classification of UHPC mechanical properties [J]. *The Chinese Highway Journal*. 2021, 34(08): 23-34.